1966

Material considerations in plastic design, November 1966 (69-25)

P. F. Adams

T. V. Galambos

LEHIGH UNIVERSITY INSTITUTE OF RESEARCH

Plastic Design in High Strength Steel

MATERIAL CONSIDERATIONS IN PLASTIC DESIGN

by

Peter F. Adams

Theodore V. Galambos

Fritz Engineering Laboratory Report No. 297.23

Plastic Design in High Strength Steel

MATERIAL CONSIDERATIONS IN PLASTIC DESIGN

by

Peter F. Adams

and

Theodore V. Galambos

This work has been carried out as part of an investigation sponsored jointly by the Welding Research Council and the Department of the Navy with funds furnished by the following:

American Iron and Steel Institute

American Institute of Steel Construction

Naval Ships Systems Command

Naval Facilities Engineering Command

Fritz Engineering Laboratory
Department of Civil Engineering
Lehigh University
Bethlehem, Pennsylvania

November, 1966

Fritz Engineering Laboratory Report No. 297.23

ABSTRACT

This report presents the results of a study of a three span beam. The study considered the spread of the yielded zones at "plastic hinge" locations by using a moment-curvature relationship which directly reflected the stress-strain curve of the material. The effect of the material properties on moment redistribution was investigated as well as the influence of the rotary cold-straightening process on the effective material properties.

TABLE OF CONTENTS

1. INTRODUCTION

This report discusses the influence of the material properties on the structural behaviour of a steel member. In particular, the ability of such a member to redistribute bending moments in the inelastic range is investigated. The investigation was initiated as part of a program to apply plastic design rules to the high strength, low alloy steels. These steels have material characteristics which are somewhat different from those observed for the low-carbon steels.(1) In addition, it has been observed that the rotary cold-straightening process may change the properties of the material.(2) (3)

The basis of the simple plastic theory is the assumption that moment redistribution can occur so that the plastic moment capacity, M_p, is reached and held at a number of locations and thus the structure can fail as a mechanism.(4) The moment-curvature (M-ϕ) relationship is assumed to be ideally elastic-plastic.(2) As a consequence, the inelastic rotations are concentrated at discrete points (hinges) which are assumed to have infinite rotation capacity. As the structure is loaded and the plastic moment is reached at successive hinge locations, discrete reductions in stiffness replace the gradual deterioration which occurs in an actual structure. This simplified treatment provides a good indication of the overall behaviour of the structure and a convenient means of determining the maximum load.(4)

To study the local behaviour in the hinge areas and to determine the actual deformation capacity of a member, an analysis must be performed which accounts for the strain hardening properties of the material and the detailed curvature distribution along the length of the member.(5)

This report presents the results of such an analysis. The structure is assumed to consist of a material with the stress-strain (σ-ϵ) relationship

shown in Fig. 1. In Fig. 1, the yield stress is denoted as σ_y and E represents the modulus of elasticity. The strain hardening modulus is denoted by E_{st}. The yield strain and the strain at the onset of strain hardening are ϵ_y and ϵ_{st}, respectively. The effect of the material characteristics is studied by varying the values of E_{st} and or ϵ_{st}. The results are discussed with the object of determining those factors which influence the abiltiy of the structure to redistribute bending moment.

The rotary straightening process is performed by cold bending the member, about its weak axis; back and forth between two sets of heavy rollers. This process induces residual stresses due to the cold bending, but more important, it may alter the effective properties of the material. This process is illustrated analytically and the predicted material properties are compared with those measured on tensile coupons cut from rotarized sections.[3]

2. ANALYTICAL MODEL

The following section presents the results of an analytical study of the influence of the stress-strain characteristics on the moment redistribution process. The problem can be stated as follows: in a structure with one hinge formed, it is desired to increase the moment at potential adjacent hinge locations while at the same time holding the strains at the original hinge location to reasonable values and, in addition, ensuring that the yielded length at this location does not reach the length required to precipitate local buckling.

The model chosen for the investigation is the three span beam shown in Fig. 2a. The member has three equal spans of length, L, and is loaded with a concentrated load, P, at the mid-point of the centre span. The beam is composed of material possessing the characteristics shown by the σ-ϵ curve of Fig. 1.

If the cross-section is assumed to be composed of two infinitely thin flanges separated by the depth of the cross-section, d, and the effect of residual stress is neglected, the moment-curvature (M-ϕ) relationship is that shown in Fig. 3.[6] In this figure M is the full plastic moment and I is the major axis moment of inertia of the cross-section. The curvature corresponding to the attainment of M_p is ϕ_p and that at the initiation of strain hardening is ϕ_{st}. The M-ϕ relationship shown in Fig. 3 is based on the assumption that instability of the cross-section does not occur.

The elastic limit curvature distribution along the length of the member is shown in Fig. 2b. As the load is increased the moment at the load point, M_c, exceeds M_p and the yielded zone spreads from the mid-span section along the length of the member. The curvature distribution at this stage

is shown in Fig. 2c. If the load is increased further, the moments at the interior supports, M_s, also exceed M_p and yielded zones begin to spread from the supports. The corresponding curvature distribution is shown in Fig. 2d.

The in-plane load-deflection behaviour of the beam will be traced using the M-Ø curve of Fig. 3. The curvature distributions shown in Fig. 2 are non-dimensionalized in such a way that the only numerical data necessary are the ratios of E/E_{st} and ϵ_{st}/ϵ_y.[3] The effect of the material characteristics will be examined by varying these two ratios.

An analysis similar to that presented here was performed by Horne.[7] An analysis which considered, in addition, the effects of gradual yielding and residual stress was given by Lay and Smith.[8] Horne considered only the effect of strain hardening on the equalization of moments at hinge locations, however, Lay and Smith were able to show that strain hardening was necessary for moment redistribution. The present paper shows the variation of P, M_s and M_c with the variation of E_{st} and ϵ_{st} over the practical range of variation of these properties. The investigation also shows the variation of the yielded length at the load point, the load point deflection and the maximum strain over the same range of variation of the material characteristics.

While the effect of the material characteristics on moment redistribution, as evidenced by idealized in-plane behaviour, is important; it has been observed that the factor which limits the rotation capacity in a braced beam under moment gradient, is local buckling of the compression flange.[9][10] This is due to the large strains existing in the portions of the member adjacent to the plastic hinges. It has been shown that to delay the occurrence of local buckling until the optimum rotation capacity has been obtained, the flange width-to-thickness (b/t) ratio must be limited

approximately to:

$$\frac{b}{t} = 2\sqrt{\frac{G'}{\sigma_y}} \qquad (1)$$

where G' is the torsional rigidity in the strain hardening range, given by:

$$G' = \frac{2G}{1 + \left[\frac{E}{4E_{st}}\right]\left[\frac{1}{(1 + \mu)}\right]} \qquad (2)$$

In equation (2), G is the elastic torsional rigidity and μ is Poisson's ratio.

For ASTM-A36 or A441 steel, which has not been previously cold worked, E_{st} is approximately equal to E/45. The limiting b/t ratio for A36 material, with σ_y equal to 36 ksi, is 17 (from Eq. (1)), and for A441 material, (σ_y = 50 ksi) the ratio is 14. If, however, E_{st} is decreased to a value of E/450, which is thought to represent a reasonable upper bound for material which has been previously yielded during the cold-straightening process, the corresponding limits on b/t are 5.5 and 4.7.

From equations (1) and (2) the effect of the strain hardening modulus, E_{st}, on the local buckling resistance of the cross-section can be determined. In order to ensure reasonable limits for the flange plate geometry in sections used for plastic design, the value of E_{st} must be as large as possible. This is particularly important with the high strength steels as an increase in σ_y will decrease the range of allowable b/t ratios. It will also be shown that a high value of E_{st} increases the efficiency of the moment redistribution process.

3. RESULTS OF ANALYSIS

Computations have been performed for two ratios of E/E_{st}; 45 and 450; and three ratios of ϵ_{st}/ϵ_y; 1, 12 and 20. The values of E_{st} were chosen to represent the material characteristics of structural steel under the conditions described above. The values of ϵ_{st}/ϵ_y were chosen to represent a bilinear material ($\epsilon_{st}/\epsilon_y = 1$) and a strain jump which is typical of the structural steels ($\epsilon_{st}/\epsilon_y = 12 - 20$). Throughout the studies in this section the strain hardening range is assumed to be linear.

The plot showing the increase in bending moments with increased load is shown in Fig. 4. This graph traces the process of moment redistribution. The load P, non-dimensionalized as P/P_p is plotted on the vertical axis, where P_p is the load predicted by simple plastic theory ($P_p = 8M_p/L$). The bending moments at the support and at the load point, M, are plotted on the horizontal axis. The moments are non-dimensionalized as M/M_p. The predictions given by an elastic-plastic analysis are shown as the dashed lines.[6] As opposed to the idealized elastic-plastic prediction, the strain hardening properties of the actual material produce an increase in the load point moment once yielding has been initiated at this point. At $P/P_p = 1.0$, the load point moment is well above M_p while that over the interior support is below M_p.

The region of interest in Fig. 4 is shown in detail in Figs. 5 and 6. In Fig. 5 the curves are plotted for $E/E_{st} = 45$ and three ratios of ϵ_{st}/ϵ_y; 1, 12 and 20. In Fig. 6 the curves are plotted for $\epsilon_{st}/\epsilon_y = 12$ and $E/E_{st} = 45$ and 450. In both cases an increase in the pertinent ratio represents an increase in the flexibility of the material. From Figs. 5 and 6 it can be seen that the more flexible materials provide more efficient redistribution

since they reach $P/P_p = 1.0$ while holding the maximum moment (at the load point) to a smaller value than do their stiffer competitors.

For further load increase, once M_p has been reached under the load, the zone of large curvatures shown in Fig. 2c must spread from the load point along the length of the beam. Simultaneously, the moment at this location, M_c, increases above M_p. Once the yielded length, τL, has reached a sufficient magnitude for a local buckle to form, the response of the member can no longer be predicted and its useful life is assumed to be terminated. The variation in τL with an increase in load is thus a critical property and is plotted in Fig. 7 for material having $E/E_{st} = 45$.

Fig. 7 plots P/P_p against the yielded length, τL, non-dimensionalized as $\tau L/L$. As shown in Fig. 7, those materials which are more flexible, that is, have larger values of ϵ_{st}/ϵ_y, will develop considerable shorter yielded lengths at the simple plastic load level ($P_p = 1.0$). Thus, the more flexible materials have a larger rotation capacity before the formation of a local buckle. The same trend was evident for those materials having smaller values of E_{st}.[3]

For wide flange shapes of compact cross-sections, the wavelength of a local buckle has been given elsewhere as 21,[11] where

$$21 = 1.42 \left(\frac{dt}{dw}\right) \left(\frac{A_w}{A_f}\right)^{1/4} d \qquad (3)$$

At the initiation of local buckling then

$$\tau_{lb} = \frac{21}{L} = 1.42 \left(\frac{dt}{dw}\right) \left(\frac{A_w}{A_f}\right)^{1/4} \left(\frac{d}{L}\right) \qquad (4)$$

In Eqns. (3) and (4), b and t denote the flange width and thickness while d and w denote the total depth of the section and the web thickness,

respectively. The area of one flange is given as A_f ($A_f = bt$) and A_w represents the web area ($A_w = w(d - 2t)$).

For wide flange sections commonly used as beams, the cross-sectional properties pertinent to local buckling have been tabulated.[12] For these sections the value of $(\frac{bt}{dw})\ (\frac{A_w}{A_f})^{1/4}$ varies from 0.50 to 0.95. Assuming that $10 \leq \frac{L}{d} \leq 30$, the resulting value of τ_{1b} varies from 0.024 to 0.145. From Fig. 7, the value of τ_{1b} required to ensure that the load can reach P_p varies between 0.044 and 0.068. Members having relatively low values of $(\frac{bt}{dw})\ (\frac{A_w}{A_f})^{1/4}$ combined with high $\frac{L}{d}$ ratios may local buckle before reaching the load predicted by simple plastic theory. This tendency towards premature local buckling is most evident in the stiffer materials, as seen in Fig. 7. For the members considered, premature local buckling will rarely occur. Even in the critical cases, the post-local buckling capacity of the flange may still enable the member to reach P_p, however, it is not possbile at the present time to evaluate this capacity.[1]

From the above considerations, it appears that the more flexible materials are more readily adaptable for use in plastically designed structures. Ideally, material should have a large value of E_{st} to provide local buckling capacity and a large value of ϵ_{st} to provide for efficient moment redistribution and to ensure that the yielded length increases as slowly as possible. The same conclusion has been reached by Lay.[13]

However, the above conclusions must be tempered by a consideration of the deflections and strains, which must be of a limited extent. Fig. 8 presents load-deflection curves for the three span beam. The plots are of P/P_p against the in-plane deflection at the load point, v, non-dimensionalized as $\frac{v}{L}\frac{1}{\sqrt{\epsilon_y}}\frac{d}{L}$ where d denotes the depth of the cross-section. Fig. 8 shows that up to the value of $P/P_p = 1.0$, the deflections are virtually the same for all materials but beyond this point, the more flexible

materials exhibit greater deformations at a given load level.

The progression of the maximum strain, ϵ_{max}, at the section adjacent to the load point is shown in Figs. 9 and 10. In these figures P/P_p is plotted against the non-dimensionalized maximum strain $\epsilon_{max}/\epsilon_y$. Fig. 9 shows the effect of increasing the length of the inelastic plateau, ϵ_{st}/ϵ_y. For the more flexible materials the maximum strain at a given load level is larger. Fig. 10 shows the same tendency for those materials having decreased values of E_{st}.

It has been argued that materials which do not possess strain hardening properties will not redistribute moments in the inelastic range.[8,14,15] However, all structural metals do exhibit strain hardening to some extent, and it has been shown that the primary effect of the reduced value of E_{st} is the lowered resistance to local buckling.[9]

It appears that the stress-strain characteristics of the structural steels make them ideally suited for their role in plastic design. The relatively large values of E_{st} (900 ksi for ASTM-A36, 750 ksi for A441) result in acceptable limits on flange geometry to prevent premature local buckling.[1,16] On the other hand the jump in strain at the yield stress (approximately 12 ϵ_y) provides a large rotation capacity while resulting[17] in a relatively short yielded length.

The conclusions above are based on a very simple model, however, in a relative sense, they are valid also for more complex structures. Presently, plastically designed structures are proportioned to provide the maximum possible rotation capacity; it is then assumed that this capacity will be sufficient to allow the structure to reach P_p. The next phase of the work remaining would consist of analyzing various structural configurations and loading conditions to determine whether this optimum rotation capacity is

indeed sufficient. A start in this direction could be provided by reanalysing the structure considered in this investigation under other loading and restraint conditions.

4. THE INFLUENCE OF COLD BENDING

The stress-strain relationship of the material, after rolling and cooling, has normally been taken as the basis of member behaviour. The influence of those portions of the member which has been locally yielded when the member was cold bent (gagged), in order to remove the initial deformations due to disturbances during the cooling process, was neglected.[7] Since the affected areas form only a small proportion of the total length of the member, the neglect of their action is justified.

In recent years the use of the rotary straightener has increased. Although it is presently limited to the smaller sections (one approximate rule of thumb is that the weak axis section modulus be less than 17) it appears that it will be used in the future for larger sections.

The rotary straightener consists of a series of heavy rolls placed as shown in Fig. 11 and used to bend the section about the weak axis. The rolls are arranged so that they bear directly on the flange-to-web junctions of the member and subject it to two complete cycles of curvature reversal; rolls No. 4 to 7 being the active, or load producing rollers. The member is fed continuously into the roller arrangement, guided by rollers No. 1, 2 and 3. Roller No. 4 is placed in a lowered position relative to the first three. The difference in elevation may vary from a fraction of an inch to several inches, depending on the size of the member, but is enough to produce a significant permanent set. Roller No. 5 then picks up the end of the member and reverses the direction of the applied curvature. The permanent set produced by this roller is approximately one-half of that produced by roller No. 4. Rollers No. 6 and 7 repeat the process with correspondingly reduced magnitudes of the applied curvature, and the remainder of the rollers act primarily as guides. The entire process is one of trial and error. The

first lengths of a given cross-section are rotarized with trial setting of the rollers. If the member is straightened in a satisfactory manner the remainder of the lengths are processed in the same way; if not, new settings are tried and the process repeated. During the process any initial curvatures virtually disappear and the final product is almost uniformly straight.

The loading situation at the time roller No. 4 is active on the member is shown (approximately) in Fig. 12a. The corresponding bending moment distribution is shown in Fig. 12b and the curvature distribution in Fig. 12c. In Fig. 12, M_y is the moment corresponding to the initiation of yielding in the extreme fibres of the cross-section and M_o is the maximum moment on the member. The corresponding curvatures are ϕ_y and ϕ_o. The complete length of the beam is subjected to the applied curvature ϕ_o as it is guided under roller No. 4 and is then unloaded elastically after passing this roller. A smaller curvature, applied in the reverse sense, is then induced by the action of roller No. 5 and so on. In order to compute the influence of this process on the member, the material behaviour under reversed loading must first be evaluated.

In order to provide a model which contains the significant features, the behaviour postulated by Chajes et al[19] and used in a modified form by Lay[20] will be adopted. This behaviour is illustrated in Fig. 13 and accounts for the unique stress-strain characteristics of the structural steels as well as (approximately) the Bauchinger effect.[21] To gain some insight into the influence of the reversed strains on the material properties, the linear strain-hardening range assumed by Lay has been replaced with a parabolic curve fitted to the initial modulus E_{st} at the initiation of strain hardening and to the ultimate stress and strain.[3] This expression accounts for the deterioration of E_{st} in the strain-hardening region.

Using these assumptions it is possible to trace the behaviour of the material through the strain reversals involved in the rotarizing process. In order to do this a sequence of applied curvatures has been selected as shown in Fig. 14. The initial curvature, ϕ_1, is $20\phi_y$, where ϕ_y is the curvature corresponding to the attainment of the yield strain at the flange tips. This is not completely arbitrary as it results in an approximate value for the deflection under the roller of 1 inch, which seems reasonable. The curvature is then reversed twice; ϕ_2 being equal to $10\phi_y$ and ϕ_3 equal to $5\phi_y$. The final applied curvature ϕ_4 is taken as $1.7\phi_y$ from a trial and error prosess which will be descirbed below. This value is required to ensure that the final configuration results in no residual curvature on the final release of moment. At this point however, there will be residual strains in the flanges, which are a result of the inelastic strains induced by the reversed bending being superimposed on those which are induced during cooling. Only the flange plate is considered in the analysis, the web is relatively unaffected.

To determine the influence of this process on the material an approximate analysis was used. The flange plate was divided into ten elements as shown in Fig. 15a and the strains induced by the applied curvatures computed at the centroid of each element. For the first applied curvature, ϕ_1, the strains in each element, ϵ, non-dimensionalized as ϵ/ϵ_y, are shown in Fig. 15b and the corresponding stresses, σ, in Fig. 15c. The stresses were calculated on the basis of a flange width of 6 inches and thickness of 0.44 inches and for material having the characteristics of A441 steel.

By integrating the stresses over the cross-section, the applied moment required to produce a curvature of $20\phi_y$ can be computed. This process is repeated for the reversals of curvature specified in Fig. 14

and for the final elastic unloading. This final unloading should produce a zero net curvature for zero applied moment. Thus the final applied curvature, ϕ_4, was adjusted to achieve this end.

During the cold bending process, each fibre of the material is assumed to behave in a manner similar to that depicted in Fig. 13. The cross-section at the end of the process is in equilibrium and has a negligible residual curvature, however, each fibre has at one time been subjected to a longitudinal strain that may be in the order of 20 or 30 ϵ_y. Thus the fibre, when strained due to the action of a superimposed external load, may behave in a bilinear manner with a much reduced strain hardening modulus. The reduction is because of the deterioration of the modulus with increased strain.

The residual stresses which result from the rotarizing process have been computed and compared with measured values.[3] The trend in the residual stress distribution induced by the rotarizing procedure can be predicted although the numerical values do not agree closely due to the uncertainties in the analysis.[3] Of much greater importance is the effect on the stiffness of the material in the strain-hardening range. Figure 15d shows the effective strain-hardening modulus, E^*_{st} plotted as a fraction of the initial modulus for the section used as an example. This is the value which would result from the strain reversals for the process shown in Fig. 14. It is obvious that the section is less stiff due to the process, but much more work remains to be done to determine fully the influence of the rotarizing process on the behaviour of plastically designed members.

Further confirmation is provided by the results of tension tests performed on specimens cut from rotarized members.[2] In addition to the assumptions made in formulating the rotarizing process and the errors in-

duced by the coarse mesh used in the numerical integration, any comparison with tension test results introduces additional difficulties associated with the location of the specimen on the cross-section. If the flange width is small, tension coupon may be cut from the material centered on the web. In this case the influence of rotarizing may be small. The other extreme would be the case of a very wide flange with the coupon cut from the material near the edge. In this case the maximum influence of rotarizing should be observed.

The tests used in this comparison are those performed on specimens cut from 12B16.5 members.[2] The flange width of this section is 4 inches and the specimens were milled from coupons located in the flange between the tip of the flange and the centre line of the web. If the rotarizing sequence described above is typical, then the material near the flange tip has undergone a process similar to that traced for element No. 1 in Fig. 14 while the material near the web remained almost completely elastic.

To simulate this case a model is postulated as shown in the inset to Fig. 16 in which half of the specimen is noted as prestrained and is assumed to have been subjected to the rotarizing sequence. The other half is noted as the virgin material.

As the model is loaded in tension, the behaviour will be elastic until the applied stress reaches the yield stress of the virgin material, σ_y. This occurs at point A in Fig. 16. At this point the virgin material will accept further strain with no increase in load, however, the prestrained material will behave in an elastic manner up to a stress of $\alpha\sigma_y$, the increased yield stress of the prestrained material. Thus the model deforms from A to B in Fig. 16 with an effective modulus of E/2. At point B the

increased yield strsss of the prestrained material is reached. To achieve any further deformation the prestrained material must be subjected to an increased stress. Due to the reduction in stiffness, as evidenced by Fig. 15d, this increased stress will be small. At point C the strain-hardening strain of the virgin material is reached and further deformation now requires a distinct increase in stress. The effective modulus is approximately three-quarters of that for the virgin material.

This is a very crude approximation to the actual behavior. It is surprising therefore to note how well tests on actual tensile specimens agree with the behavior postulated for the model.[2]

The strain-hardening modulus for 12B16.5 Section was measured for eight flange specimens and four web specimens. The original load strain curves taken for specimens X, Y, and Z are reproduced in Fig. 17. At this cross-section all three tensile specimens were loaded into the strain hardening range and the measurements necessary to determine the strain hardening characteristics were taken.

Specimen Y was cut from the web of the section and exhibits the sharp upper yield point and significant strain hardening modulus usually associated with the structural steels. The modulus computed for this specimen was 680 ksi. On the other hand spcimens X and Z exhibit a rather rounded knee and a reduced strain-hardening modulus. The areas of interest are emphasized by the arrows in Fig. 17. Although the rounded knee of the load-strain diagram can be caused by influences other than cold-bending[22] it is gratifying to note the close agreement between the behavior predicted by the model used for Fig. 16 and the flange specimens of Fig. 17.

For the other cross-sections used in the investigation of Ref. 2, the results were similar. In each case where comparison was possible the strain hardening modulus for the web specimen was approximately one third greater

than the average for the flange specimens.

In summary, for sections which have been straightened by rotarizing, the effective material characteristics (assuming the flanges to exert the dominant influence) are those of a bilinear material having an effective value of E_{st} which is decreased from that measured for the virgin material. The effect of this process is to reduce the lateral and local buckling capacity of the member.[17]

Tentatively, it appears that the stiffness reduction due to rotarizing may be in the order of 30%. More detailed information must be obtained, however, before a firm conclusion can be reached. Studies should be initiated to define, in a statistical manner, the magnitudes of the curvature reversals which may be expected during rotarizing. Along with this data, a knowledge of the behaviour of the material when subjected to large reversals of strain is essential. Finally, tests must be performed on members which have been rotarized in order to provide a check on the structural behaviour.

5. SUMMARY AND CONCLUSIONS

This report has examined the influence of the stress-strain characteristics of the material on moment redistribution in the inelastic range. In particular the important role played by the strain-hardening portion of the stress-strain curve has been emphasized.

It may be concluded that a definite strain hardening range is necessary to ensure moment redistribution. Within certain limits, the ideal material for a plastically designed structure is that which possesses a large value of E_{st} to ensure realistic limits on the flange plate geometry to preclude premature local buckling and, in addition, possesses a large value of ϵ_{st} to provide a large rotation capacity for a given yielded length.

The structural steels seem ideally suited for their role in plastic design since they possess the desired values of E_{st} and ϵ_{st}. For the structural steels, local buckling rather than material failure is the cause of rotation capacity termination. Fortunately, a high value of E_{st} leads to both a large local buckling capacity and an increase in the efficiency of moment redistribution.

Finally the report has examined the influence of the rotary straightening porcess on the effective material properties. It is concluded that the severe strain reversals produced by this process force the material to act as a bilinear material. The result is a marked decrease in the strain hardening modulus. The analysis of this process is supported by the results of recent coupon tests taken from rotarized members. No quantitative conclusions can be drawn, however, it is felt that the effect of the rotary straightening process explains the apparently reduced deformation capacity observed in some recent tests.[2] More research must be performed to fully determine the effect of rotarizing on structural behaviour.

6. ACKNOWLEDGEMENTS

This study is part of a general investigation "Plastic Design in High Strength Steel" in progress at Fritz Engineering Laboratory, Lehigh University. Dr. L. S. Beedle is Director of the Laboratory and Dr. L. W. Lu is the Project Director. The investigation is sponsored jointly by the Welding Research Council, and the Department of the Navy, with funds furnished by the American Institute of Steel Construction, American Iron and Steel Institute, Naval Ships Systems Command, and Naval Facilities Engineering Command. The Column Research Council acts in an Advisory capacity. Mr. S. L. Phillips of the Bethlehem Steel Company provided information on the rotarizing process.

7. NOMENCLATURE

E modulus of elasticity

E_{st} strain hardening modulus

E^*_{st} effective strain hardening modulus (after cold bending)

I major axis moment of inertia

L length

M bending moment

M_p plastic moment capacity

M_o maximum moment on member

P load

P_p load predicted by simple plastic theory

d depth of cross-section

v deflection

α proportionality constant (stress)

ϵ strain

ϵ_y yield strain ($\epsilon_y = \sigma_y/E$)

ϵ_{st} strain at onset of strain hardening

σ stress

σ_y yield stress

ϕ curvature

ϕ_p curvature corresponding to attainment of M_p, assuming ideally elastic behaviour ($\phi_p = M_p/EI$)

ϕ_{st} curvature at onset of strain hardening

τL yielded length, that length over which M exceeds M_p

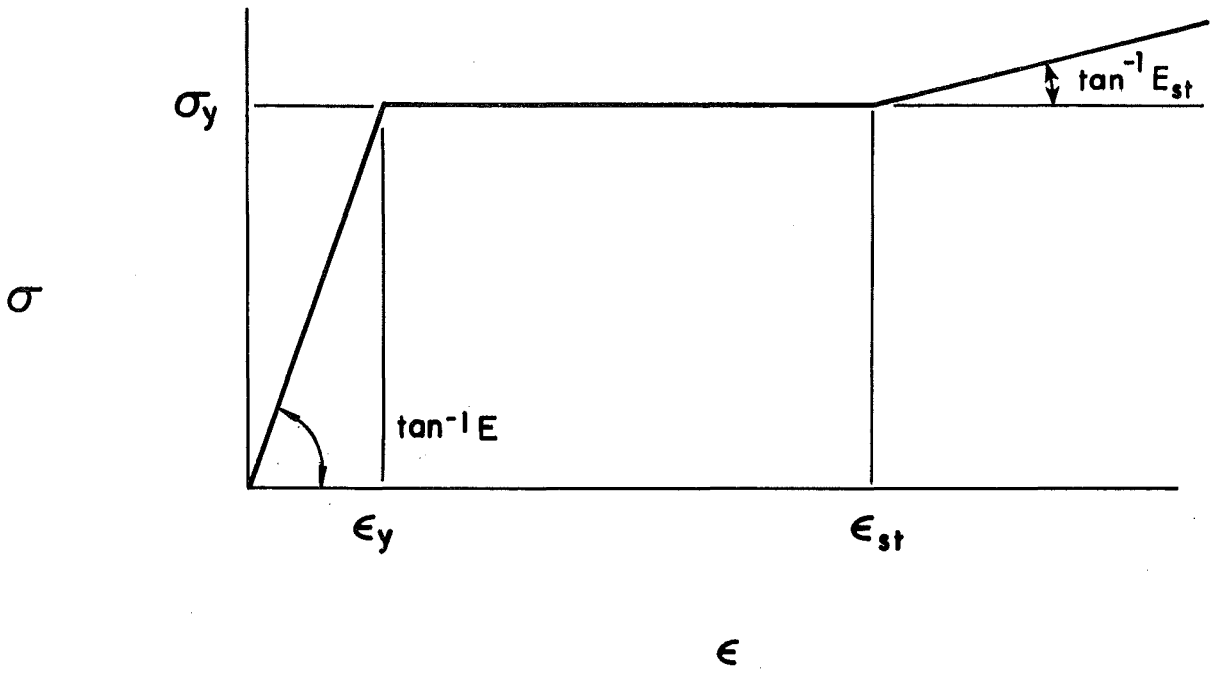

Fig. 1 Stress-Strain Diagram

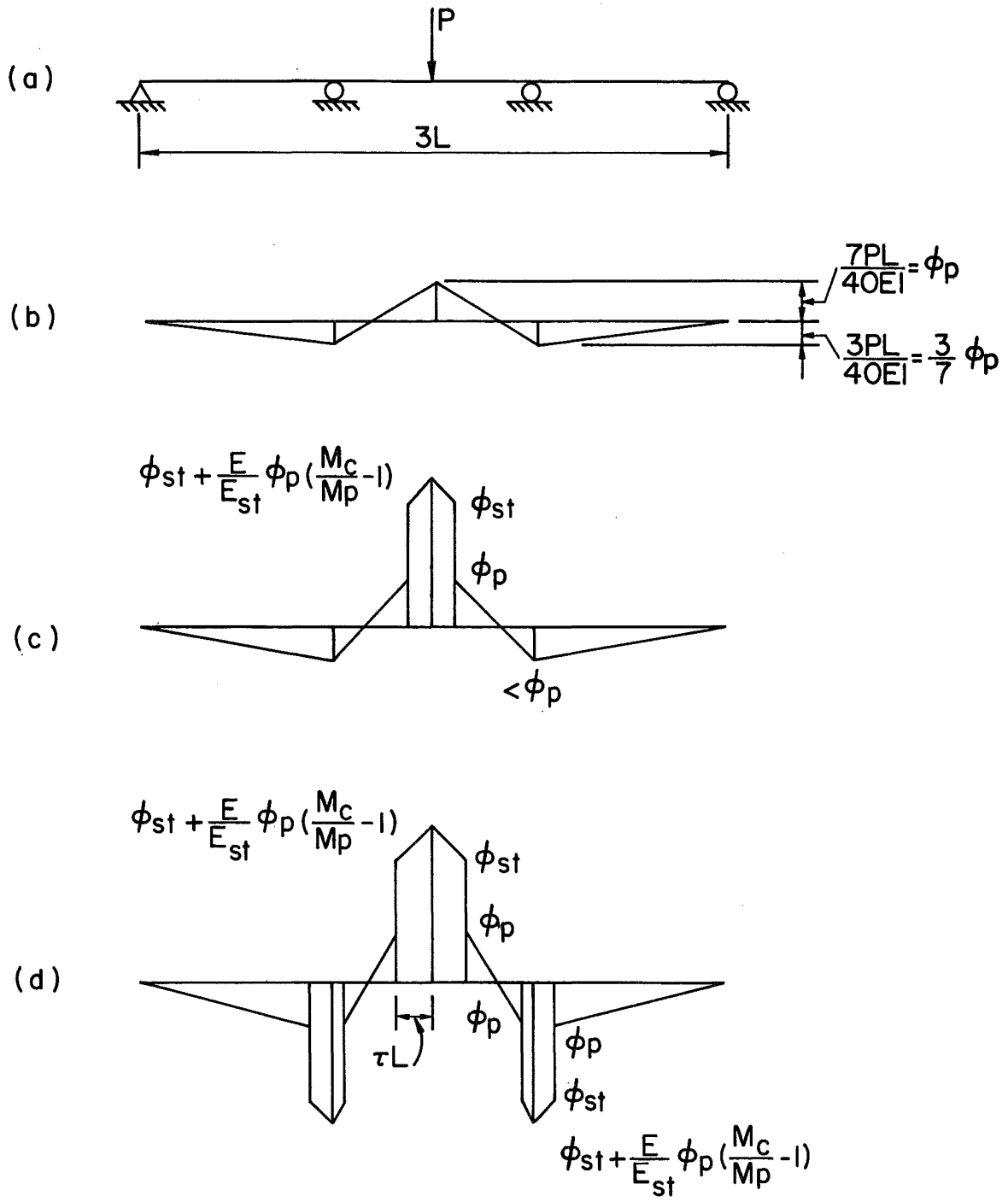

Fig. 2 Three Span Beam

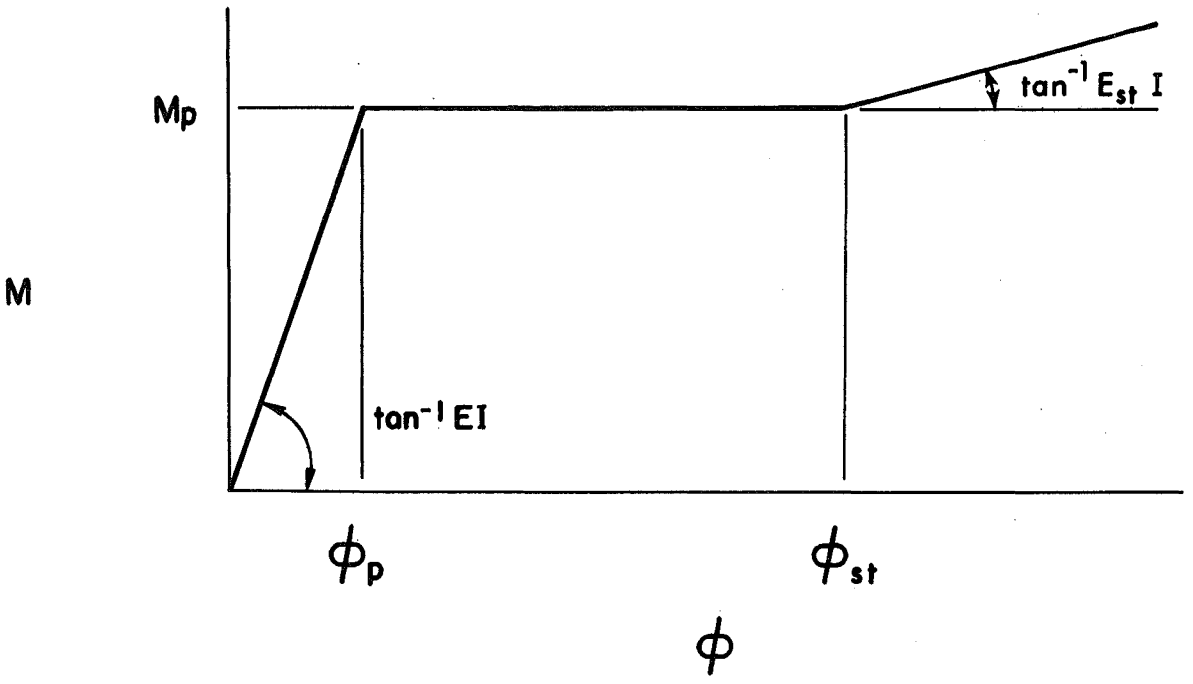

Fig. 3 Moment-Curvature

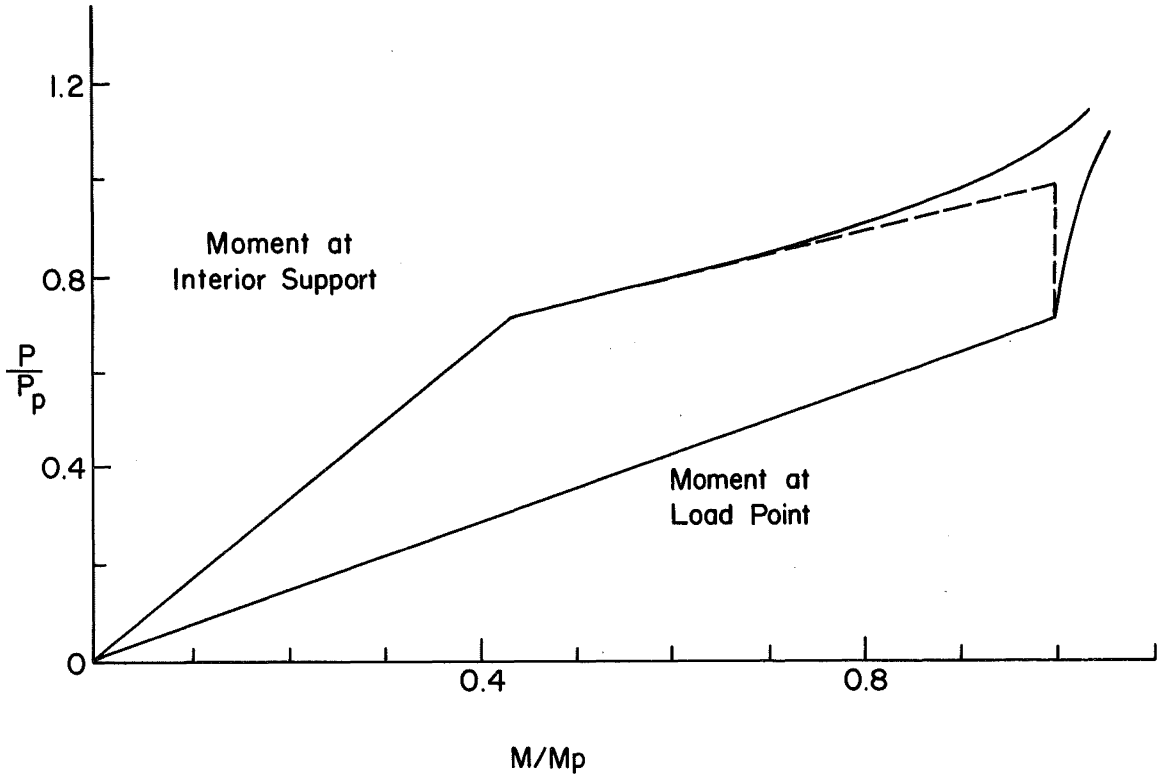

Fig. 4 Load-Moment Curves

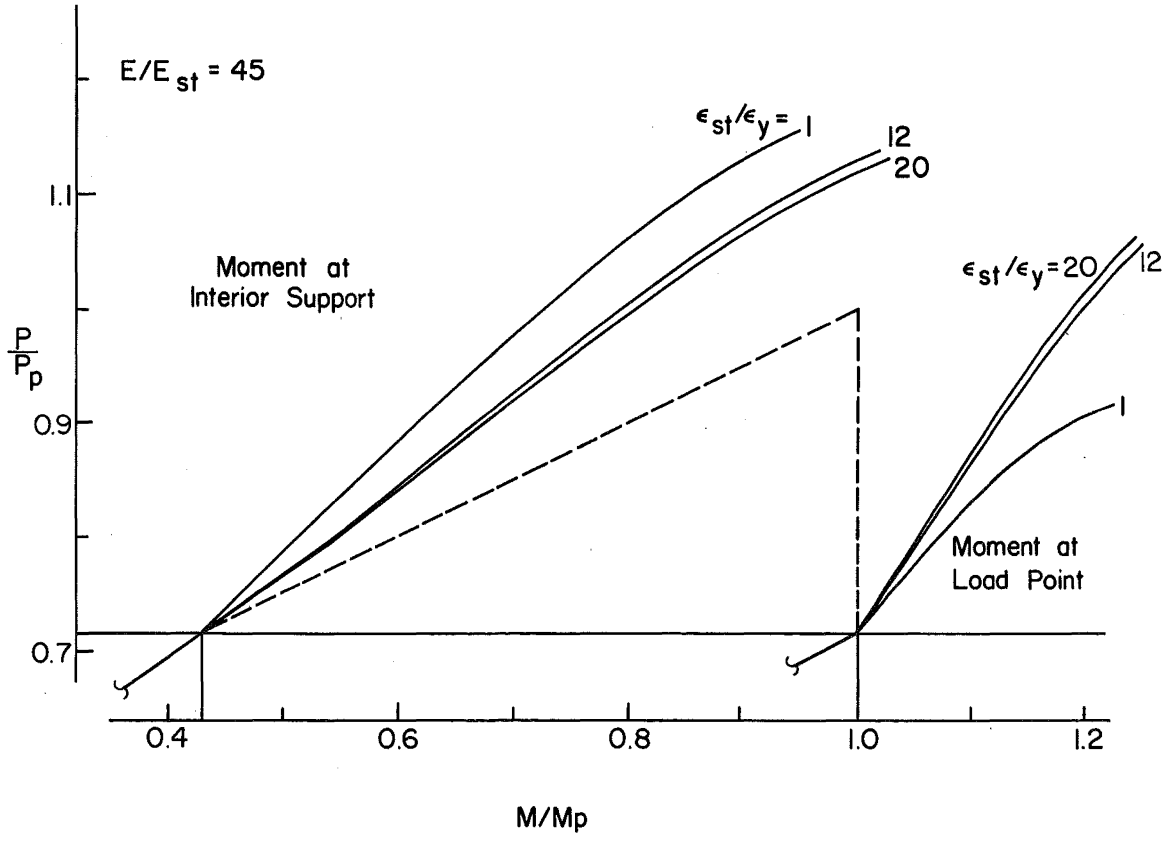

Fig. 5 Load-Moment Curves - Varying ϵ_{st}/ϵ_y

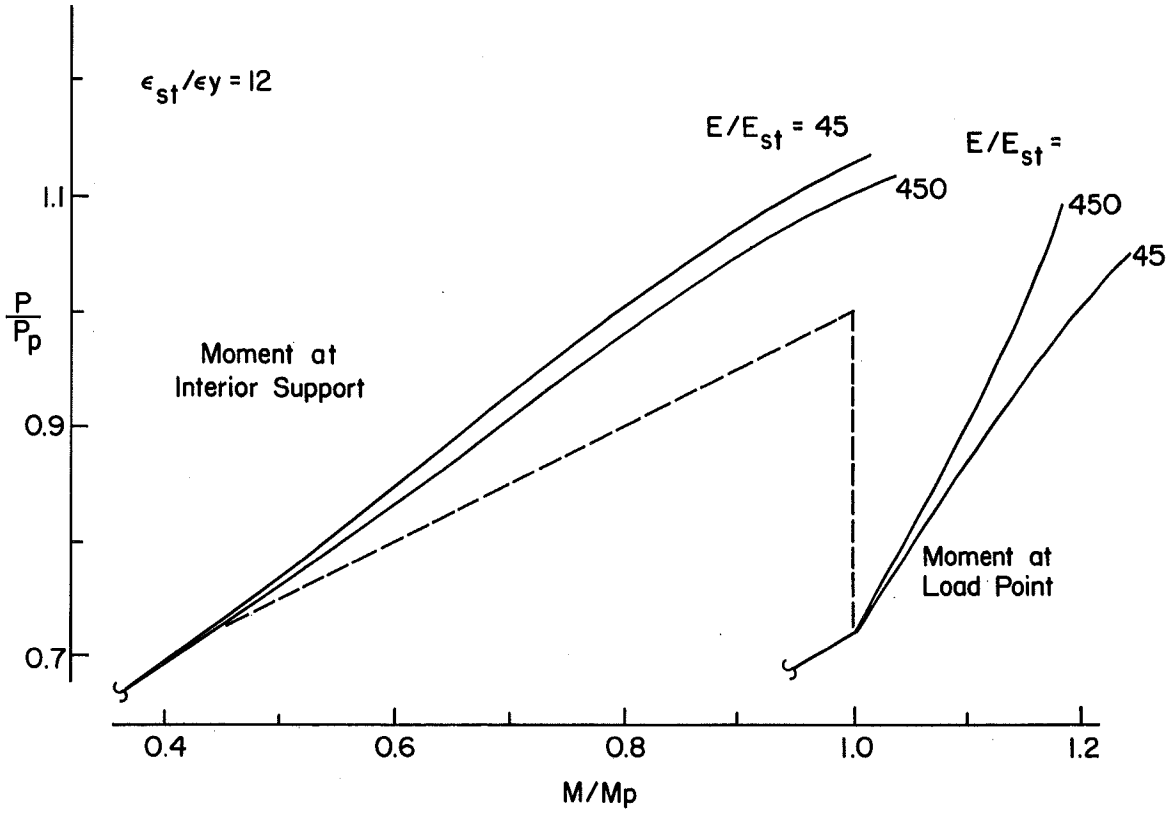

Fig. 6 Load-Moment Curves - Varying E/E_{st}

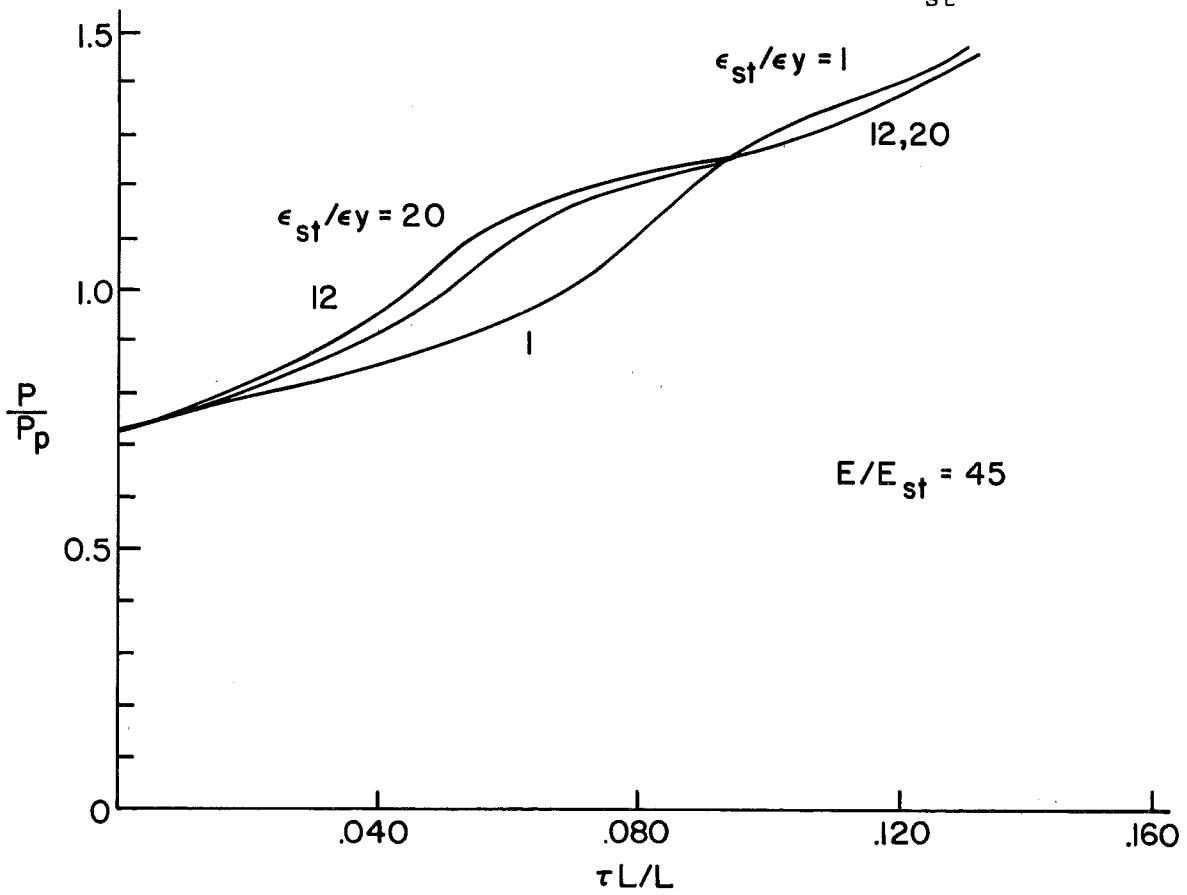

Fig. 7 Load-Yielded Length Curves

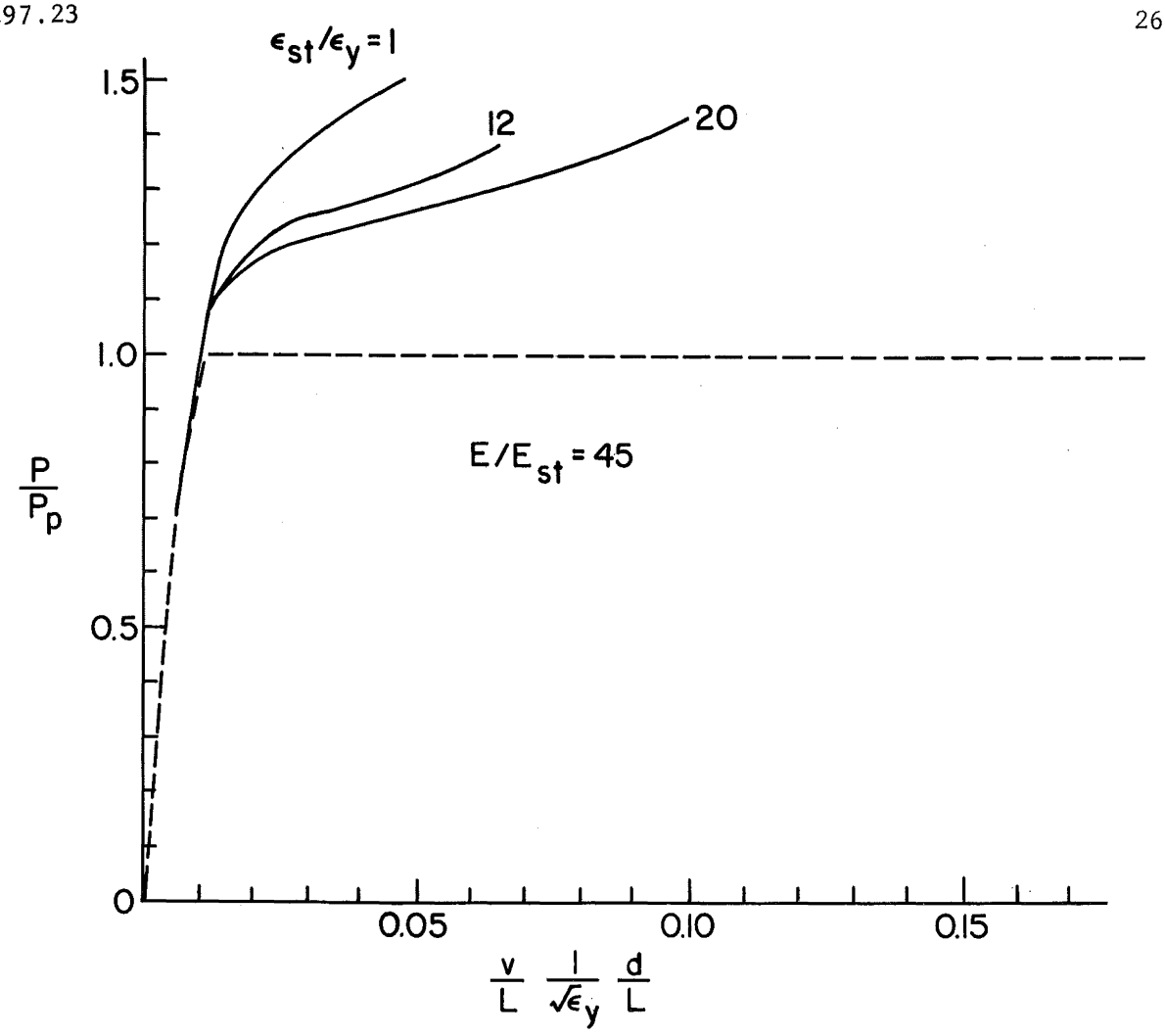

Fig. 8 Load-Deflection Curves

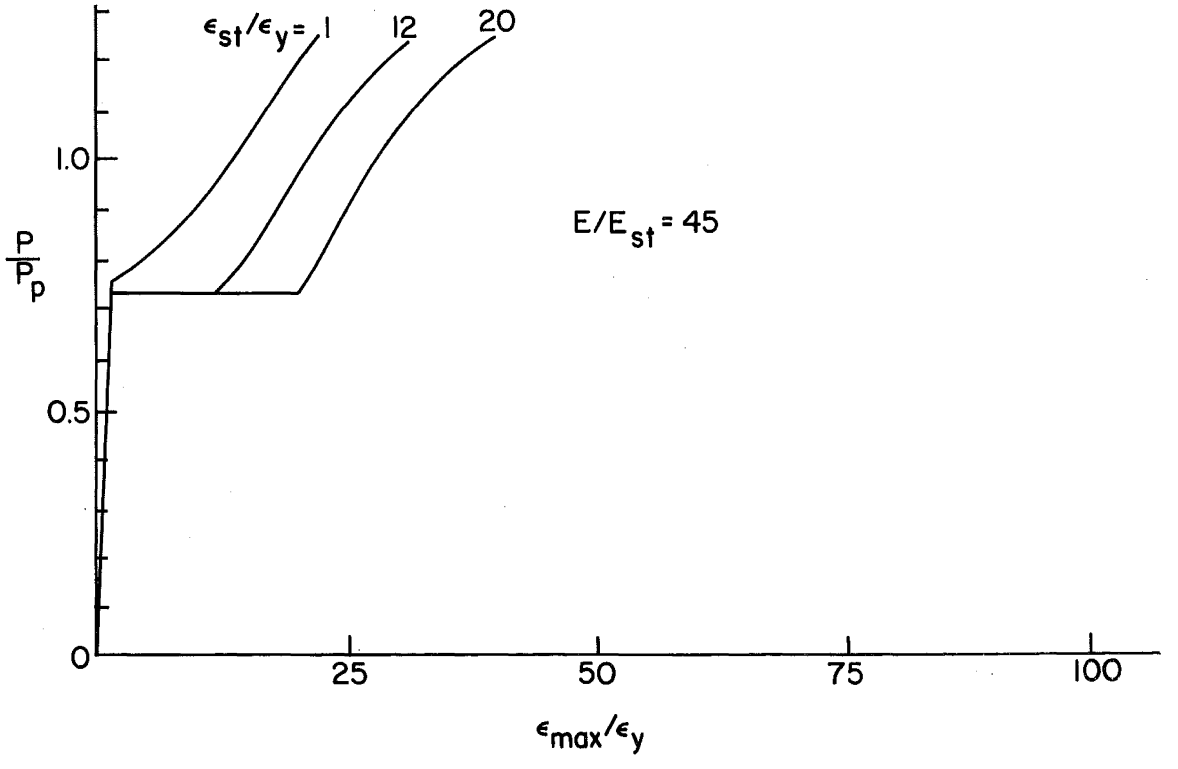

Fig. 9 Load-Strain Curves - Varying ϵ_{st}/ϵ_y

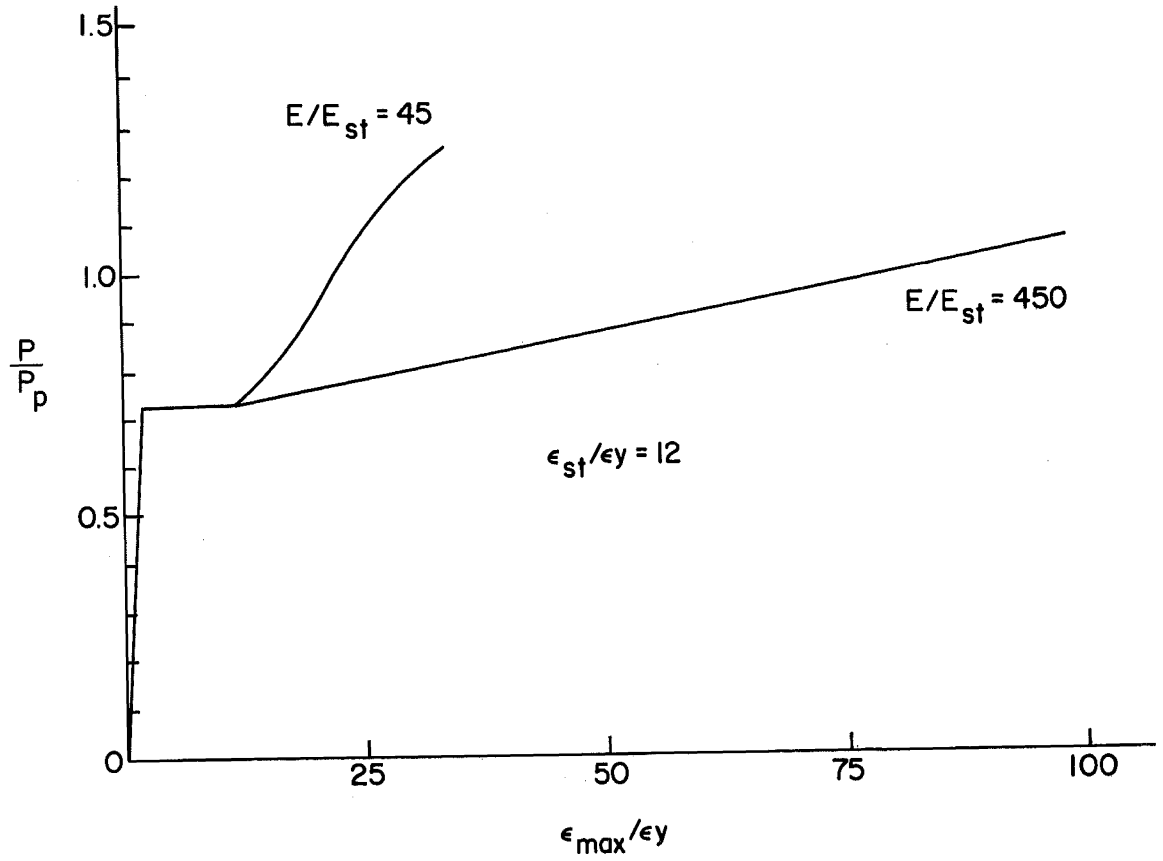

Fig. 10 Load-Strain Curves - Varying E/E_{st}

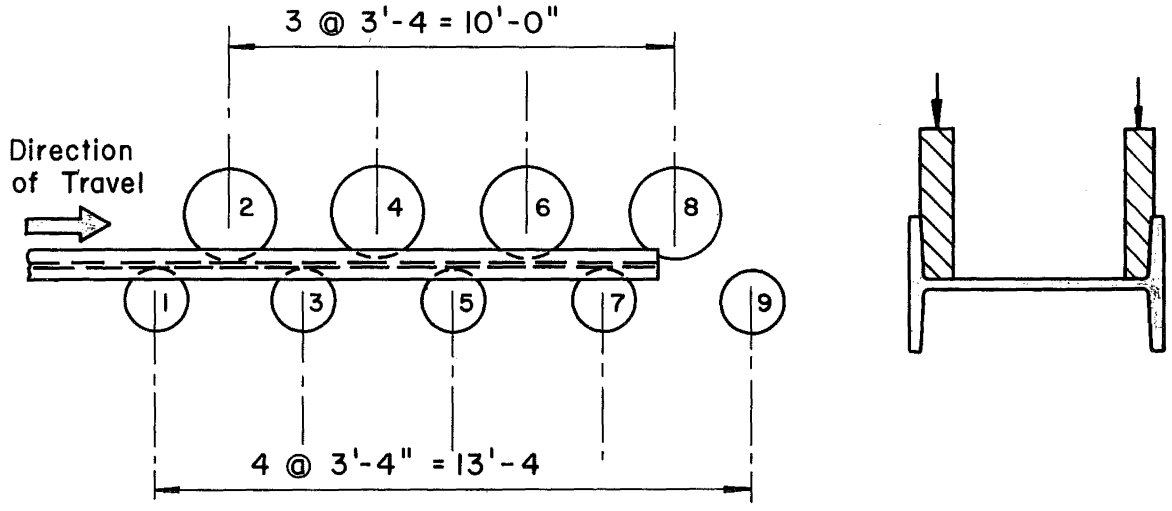

Fig. 11 Rotarizing Process

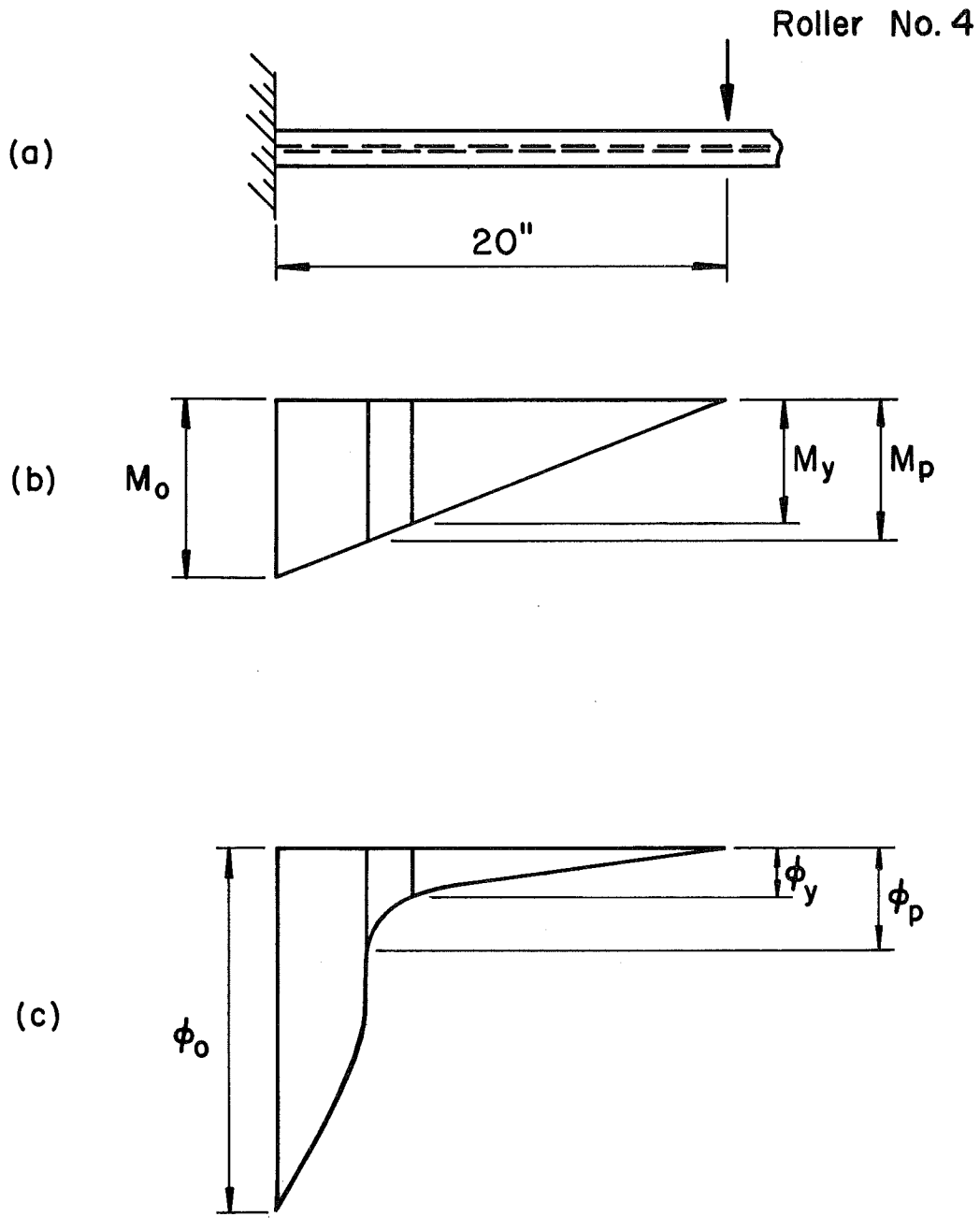

Fig. 12 Roller Loading

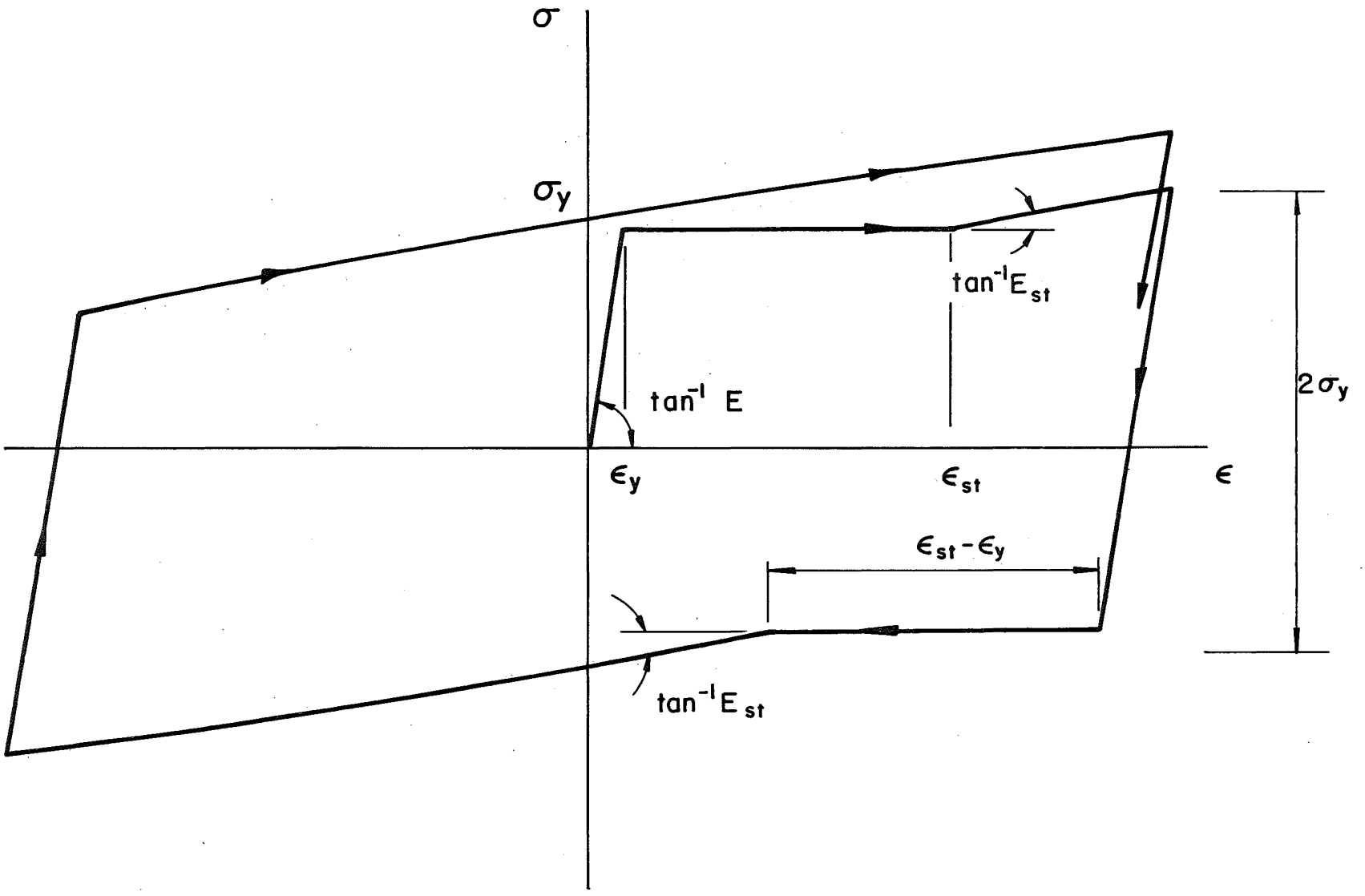

Fig. 13 Stress-Strain Diagram

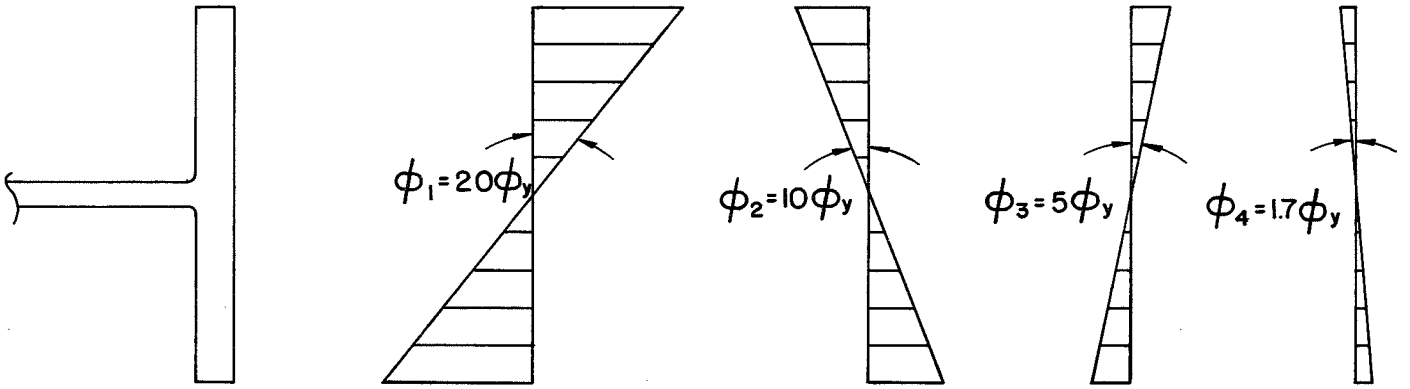

Fig. 14 Sequence of Curvatures

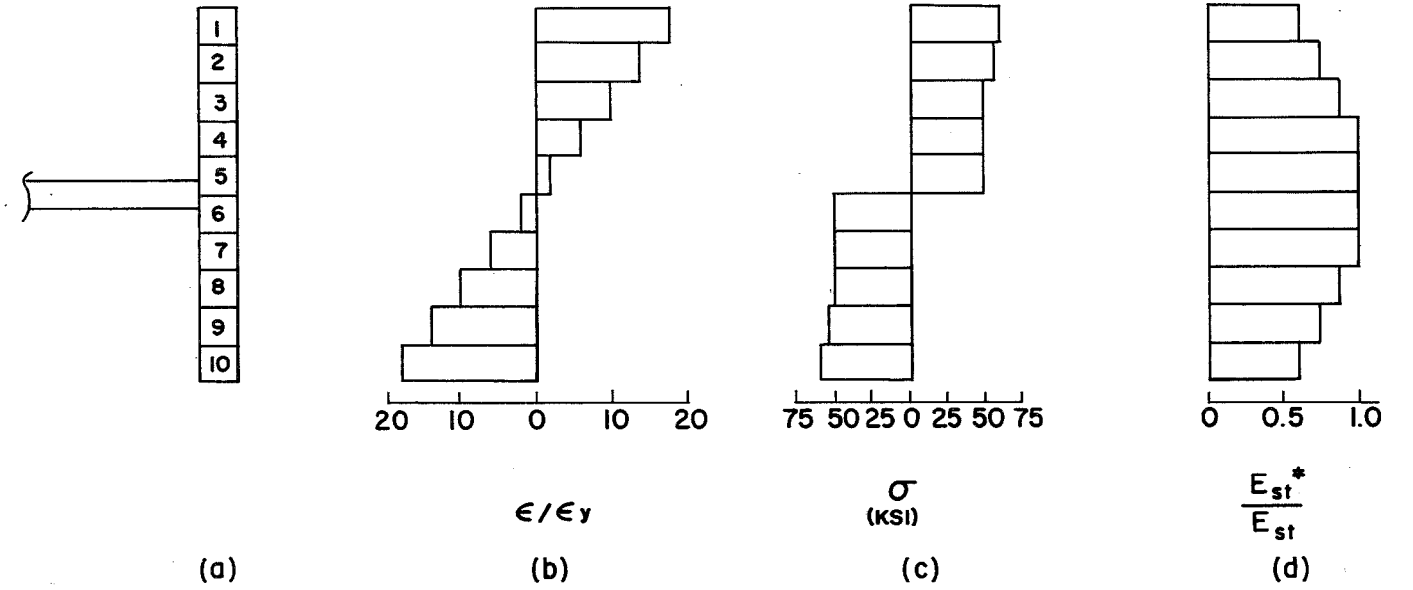

Fig. 15 Integration Process

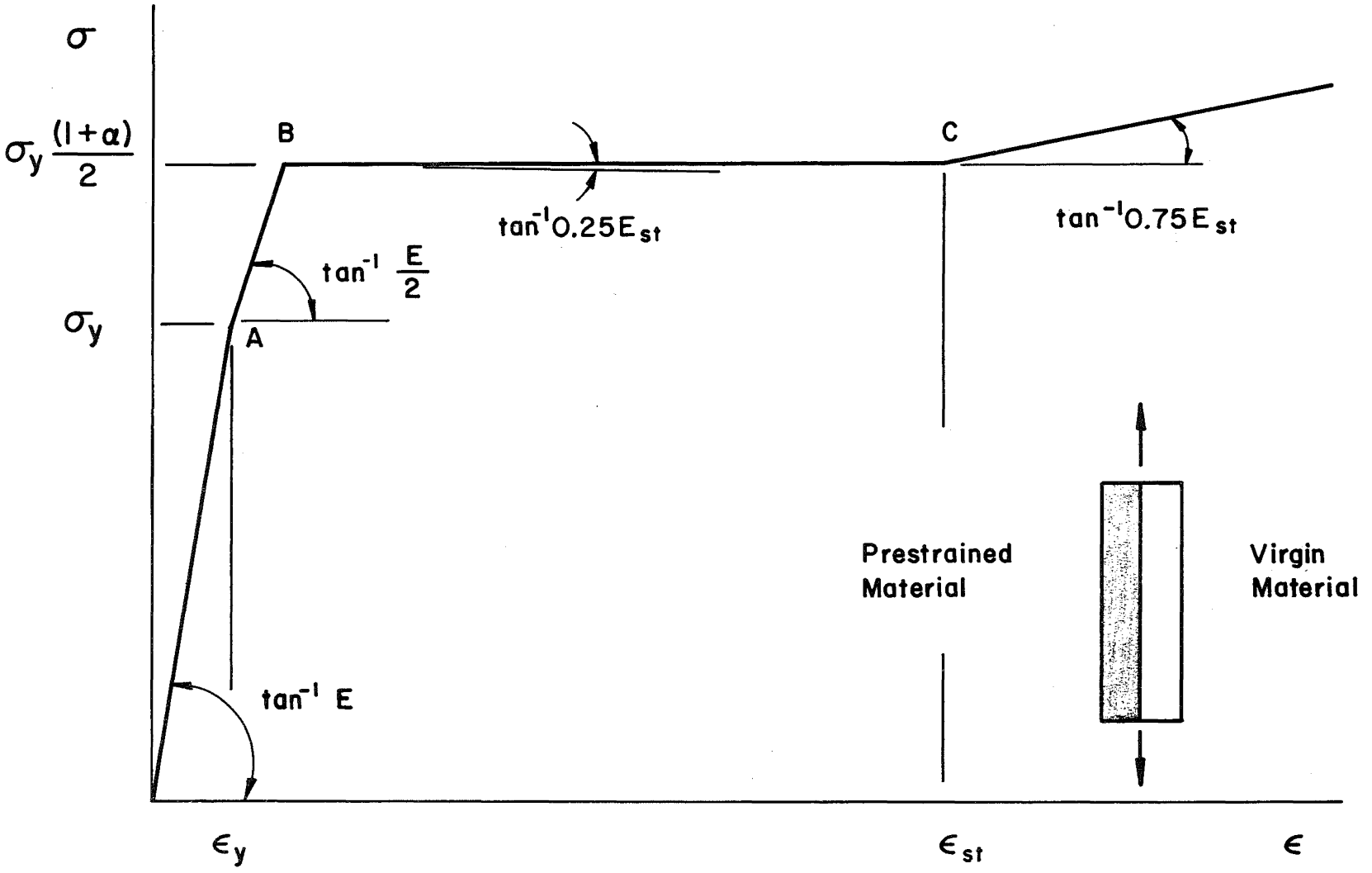

Fig. 16 Tension Specimen Model

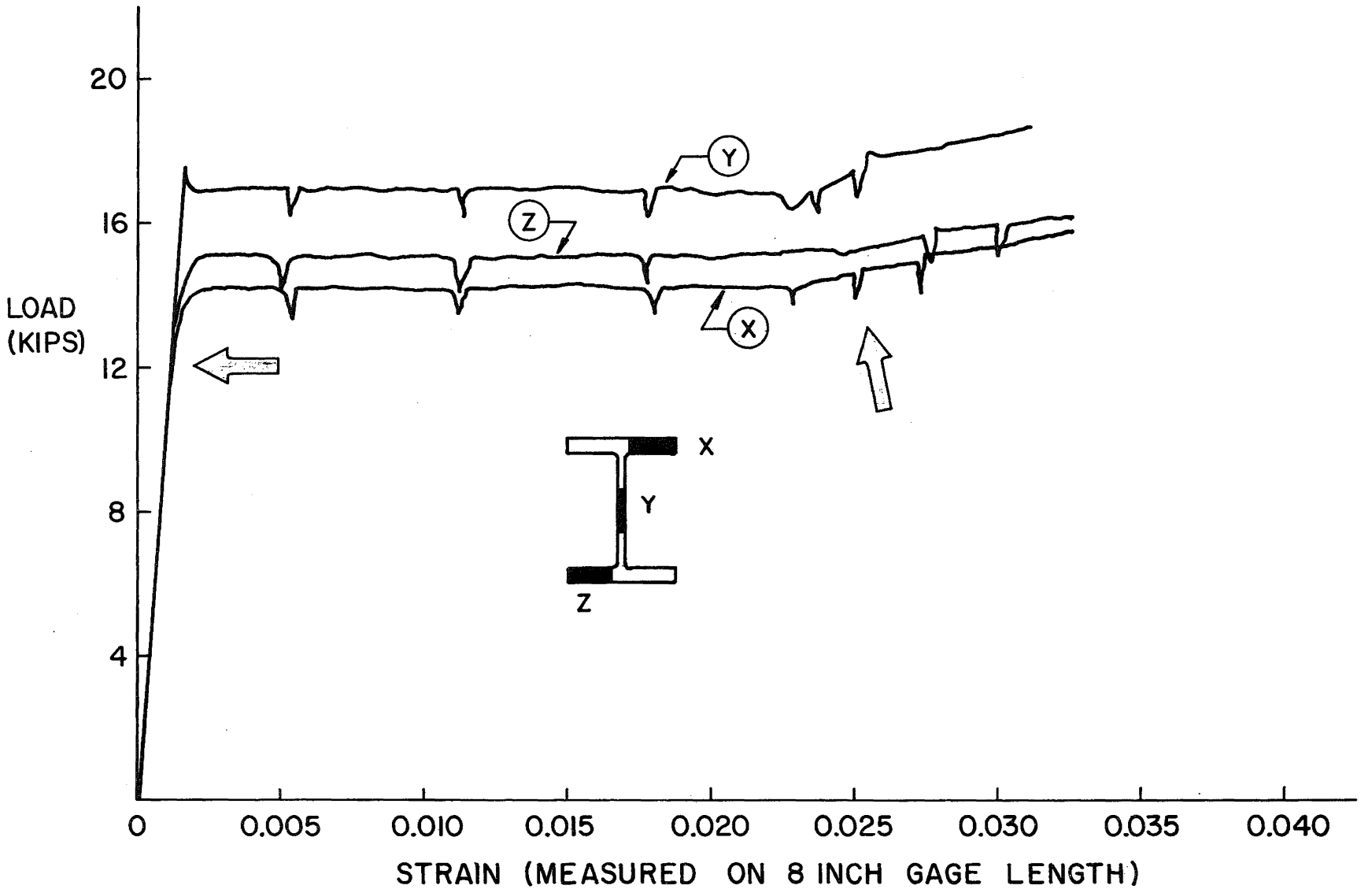

Fig. 17 Load-Strain Curves

8. REFERENCES

1. Adams, P. F., Lay, M. G. and Galambos, T. V.: Experiments on High Strength Steel Members, Welding Research Council Bulletin No. 110, November 1965.

2. Yura, J. A.: The Strength of Braced Multi-Story Steel Frames, Fritz Laboratory Report No. 273.28, September 1965.

3. Adams, P. F.: Plastic Design in High Strength Steel, Fritz Laboratory Report No. 297.19, Lehigh University, May 1966.

4. Beedle, L. S.: Plastic Design of Steel Frames, John Wiley & Sons Inc., New York, 1958.

5. Lay, M. G. and Galambos, T. V.: The Inelastic Behaviour of Beams Under Moment Gradient, Fritz Laboratory Report No. 297.12, July 1964. Accepted for publication by ASCE, July 1966.

6. Yang, C. H.: The Plastic Behaviour of Continuous Beams, Thesis presented to Lehigh University, Bethlehem, Pa. in 1951, in partial fulfillment of the requirements for the degree of Doctor of Philosophy.

7. Horne, M. R.: The Effect of Strain-Hardening on the Equalization of Moments in the Simple Plastic Theory, British Welding Research Association FE.1 - Committee on Load Carrying Capacity of Frame Structures, September 1949.

8. Lay, M. G. and Smith, P. D.: Role of Strain-Hardening in Plastic Design, Proc. ASCE, Vol. 91, ST3, June 1965.

9. Adams, P. F. and Galambos, T. V.: Discussion of Importance of Strain-Hardening in Plastic Design, Proc. ASCE, Vol. 92, ST2, April 1966.

10. Lay, M. G. and Galambos, T. V.: The Inelastic Behaviour of Beams Under Moment Gradient, Fritz Laboratory Report No. 297.12, July 1964.

11. Lay, M. G.: Flange Local Buckling in Wide-Flange Shapes, Proc. ASCE, Vol. 91, ST6, December 1965.

12. Kerfoot, R. P.: Rotation Capacity of Beams, Fritz Laboratory Report No. 297.14, March 1965.

13. Lay, M. G.: A New Approach to Inelastic Structural Design, Proc. ICE, London, England, May 1966.

14. Hrennikoff, A. P.: Theory of Inelastic Bending with Reference to Limit Design, Trans, ASCE, Vol. 113, p. 213, 1948.

15. Hrennikoff, A. P.: Importance of Strain-Hardening in Plastic Design, Proc. ASCE, Vol. 91, ST4, August 1965.

16. Haaijer, G.: Plate Buckling in the Strain-Hardening Range, Proc. ASCE, Vol. 83, EM2, April 1957.

17. Galambos, T. V.: Beams, Lecture Notes on Plastic Design of Multi-Story Frames, Chapter 3, Fritz Laboratory Report, 273.20, Lehigh University, 1965.

18. Ketter, R. L., Kaminsky, E. L. and Beedle, L. S.: Plastic Deformation of Wide-Flange Beam-Columns, Trans, ASCE, Vol. 120, 1955, p. 1028.

19. Chajes, A., Britvec, S. J. and Winter, G.: Effect of Cold-Straightening on Structural Sheet Steels, Proc. ASCE, Vol. 89, ST2, April 1963.

20. Lay, M. G.: Discussion of Effect of Large Alternating Strains on Steel Beams, Proc. ASCE, Vol. 91, ST4, August 1965.

21. Freudenthal, A.: The Inelastic Behaviour of Engineering Materials and Structures, John Wiley & Sons, Inc., New York, N. Y., 1950.

22. Beedle, L. S. and Tall, L.: Basic Column Strength, Proc. ASCE, Vol. 86, ST7, July 1960.